Investigation of ion migration in perovskite solar cells based on photovoltage/current transient

M. X. LI[1], G. L. LIU[1,2], X. Xi[1,2,*], L. WANG[1,3], Q. Y. SUN[1], B. J. ZHU[4], H. Q. ZHOU[5, 6]
[1]School of Science, Jiangnan University, Wuxi, Jiangsu, 214122, China
[2]International Joint Research Center for photoresponse functional molecular materials, Wuxi, Jiangsu, 214122, China
[3]School of Internet of Things Engineering, Jiangnan University, Wuxi, Jiangsu, 214122, China
[4]Wuxi Institution of Supervision & Testing on Product Quality, Wuxi, Jiangsu, 214101, China
[5]Zhejiang Beyondsu PV CO., LTD., Huzhou, Zhejiang, 313200, China
[6]Zhejiang Beyondsun Green Energy CO., LTD., Huzhou, Zhejiang, 313200, China

The hysteresis effect due to ion migration has become an obstacle for the development of perovskite solar cells, which means the detection of carrier properties of ion migration in perovskite devices is an urgent mission. In this article, we have proposed a novel method based on the photovoltage/current transient to evaluate the differential capacitance of the perovskite devices and calculated the charge of ion migration, confirmed that light has a facilitating effect on ion migration. Dislike contact method, the light injection way has advantages of noncontact and fast in detection, which can be applied in the rapid characterization of perovskites.

1. Introduction

In recent years, perovskite solar cells have been developed rapidly. In 2009, the first report of a liquid electrolyte-based perovskite solar cell with a power conversion efficiency of 3.8% was presented by Miyasak [1]. In 2011, Park has achieved a power conversion efficiency of 6.5% by using a highly concentrated perovskite precursor solution [2]. Today, the power conversion efficiency of perovskite solar cell has exceeded 25% [3]. Due to the explosive development, perovskite solar cells are now the hottest field in the community photovoltaics.

However, perovskite solar cells are facing poor stability and strong hysteresis (the phenomenon of non-overlapping *J-V* curves) [4-6], which is fundamentally because perovskite material itself of ionic property. Because the ionic bonds inside, the ions can easily attract water thus trigger the degradation of perovskite crystal. Because of the fragile property of perovskite, the source of the hysteresis effect has many assumptions, and the current theoretical conjectures of the cause of the hysteresis effect of perovskite solar cells are mainly the following three: (1) ferroelectricity [7] (2) charge trapping and defects [8] (3) ion migration [9]. With the development of theories, ferroelectricity has been gradually excluded as the cause of the hysteresis effect of perovskite solar cells, while recent experiments and simulations are revealing that charge trapping and defects

and ion migration play a significant role in the hysteresis effect of perovskite solar cells [10-12]. Simulations were carried out by Atul Kumar indicated that ion migration in the perovskite absorber layer is one of the reasons associated with the *J-V* hysteresis observed in perovskite solar cells [13]. To further link the ion migration, Li has introduced an external bias voltage and to modulate the charge and electric field of the cell in their experiments, it was finally demonstrated that the defects generated by ion migration, which has enlarged the hysteresis difference [14]. S. Meloni applied different bias voltages to the perovskite solar cell and measured the current density-voltage (*J-V*) curves of the perovskite solar cell under different conditions [15], they further demonstrated that the appearance of the hysteresis effect is related to the ion migration rather than the ferroelectric effect.

Based on previous research, it was found that the hysteresis effect was strongly related to ion migration inside the perovskite during scanning [16-18]. Contrast to the carrier migration, the ion migration mainly relies on the inertance of ions. Hence the ionic current was slower than charge current when tuning the electric filed inside of solar cells. To enhance the understanding of hysteresis, an accurate characterization of ion migration within perovskite solar cells is expected. Kang has proposed that Kelvin Probe Force Microscopy (KPFM) can monitor ion migration in perovskite solar cells [19]. Meanwhile, Yun separated and collected the charges on the grain boundaries of $CH_3NH_3PbI_3$ thin films with

$CH_3NH_3PbI_3/TiO_2/FTO/glass$ heterojunction structure by using KPFM and c-AFM, confirmed the beneficial role of grain boundaries in efficient carrier collection [20]. Liu directly observed $CH_3NH_3^+$ and I^- migration in $CH_3NH_3PbI_3$ by using time of Flight-Secondary Ion Mass Spectrometry (TOF-SIMS), revealed that the hysteresis effect was associated with $CH_3NH_3^+$ and I^- migration [15, 21]. However, these detection have several drawbacks as follows: (1) different to perovskite films, perovskite solar cells have their own functional layers such as hole transport layer, electron transport layer, metal cathode, and conductive glass [22-24], and these detection mentioned above are contact measurements, which are difficult to measure the encapsulated perovskite solar cells; (2) Perovskite are ionic crystals with low dissociation energy, and contact measurements are difficult to eliminate potential stress on perovskite crystals, resulting in inaccurate measurement results; (3) These measurement methods are difficult to conduct quantitative studies which cannot explain ion migration in details. In general, it is difficult to characterize solar cells based traditional methodologies for perovskite films.

Photovoltage/current transients are time-resolved measurement technique used to study the carrier recombination process in solar cells [25], which is based on small signal modulation of the incident light with low power of pulse laser to excite the dynamic of open-circuit voltage (V_{oc}) of the solar cells. The V_{oc} directly related to the quasi-Fermi level [26]. It is mainly used in the measurement of defect states. TPC can extract the charge from the solar cells [27], and TPV can determine the electron recombination lifetime of solar cells [10, 28-29]. And, in contrast to the above-mentioned test method, it is a non-contact measurement which has slight effect on films.

In this article, we have applied photovoltage/current transient (TPV/TPC) methodology to characterize the ion migration inside of perovskite solar cells. We obtained the differential capacitance of the solar cell by combining the charge extracted from the TPC with the carrier recombination lifetime extracted from the TPV, which can reflect the degree of ion migration. By analyzing the differential capacitance of the perovskite solar cell under different conditions, we calculated the concentration of ion migration from the perovskite solar cell under a specific light exposure. Based on transient methodology, we have a chance to extract ion migration from charge transportation in details.

2. Experiments

The experimental object of this paper is a planar heterojunction structure MAPbI$_3$ perovskite solar cell prepared by two-step spin-coating method. It was prepared as follows: The ITO glass substrate is first washed with deionized water, acetone and ethanol for 20 minutes. Afterwards, they were soaked in isopropyl alcohol (IPA), then dried using an air compressor and treated with ozone

and UV light for 20 minutes. The ITO substrate was spin-coated twice at 3000 rpm to deposit a dense SnO_2 layer for 30 s and annealed at 150 °C for 15 min in air with a 1:10 ratios of SnO_2 solution to ultrapure water. The perovskite films were prepared using a stepwise method in which 461 mg of PbI_2 and 80 mg of MAI were dissolved in DMSO/DMF to prepare the precursor solution, and the precursors were spin-coated in a glove box at 3000/30 rpm with 0.4 ml of chlorobenzene added dropwise during spin-coating. After spin coating, the layers were annealed at 150 °C for 15 min. Spiro-OMeTAD was then used as the HTM layer, and the Spiro-OMeTAD /chlorobenzene (75 mg ml^{-1}) solution consisted of the addition of 35 μl Li-TFSI/acetonitrile (260 mg ml^{-1}) and 30 μl 4-tert-butylpyridine deposited by spin coating at 3500 rpm for 30 s. The device was accomplished by thermal evaporation of gold under vacuum. The active layer of perovskite solar cells was 0.0908 cm^2.

Standard current/voltage (J-V) measurements are performed at solar background light (AM 1.5) using a standard solar simulator. J-V measurements are typically shown below. First, the cell is aligned in the simulator, then running the Solar Simulator to apply continuous bias voltage to the solar cell and record voltage/current data with the Keithley 2400 sourcemeter.
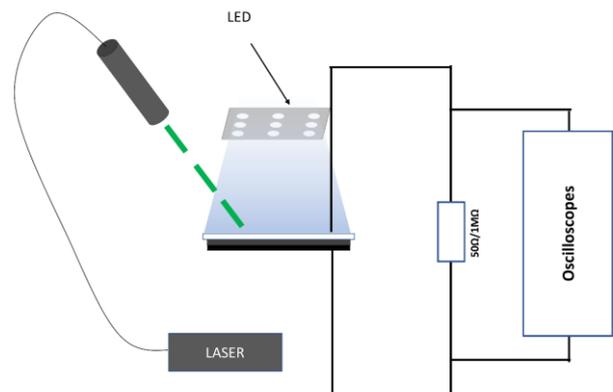

Fig. 1. Schematic diagram of the experimental device

The process of photovoltage transient and photocurrent transient measurement is controlled by an ARM chip. Its background light source of white LED can be powered up to 10 W, supply by a DC-DC current source. The current output level of the current source is controlled by the ARM receiving ADC feedback to change the DAC of the ARM chip. The ARM chip can control the intensity of the background light by this way. The perturbation source semiconductor laser has a wavelength of 532 nm and a power of 30 mW. The pulse is controlled by a fast solid-state switch with a pulse frequency of 50 Hz and a fall time of 1 ns for the pulse. The measurements are highly accurate because the low power and short perturbation time of the semiconductor laser make it cannot affect the solar cell steady state. The data is

acquired by using a PicoScope 2208 oscilloscope with 8-bit accuracy and 100 MHz analog bandwidth.

Photovoltage transient technology is similar to photocurrent transient technology, only minor differences in experimental design, that is, the perovskite solar cell remains open circuit in the photovoltage transient test and the photocurrent transient test in the perovskite solar cell keep short circuit condition. The photocurrent transient technique can measure the current response of a solar cell under short-circuit conditions and thus estimate the charge present in the solar cell and use it to perform differential capacitance analysis to derive the charge density in the solar cell.
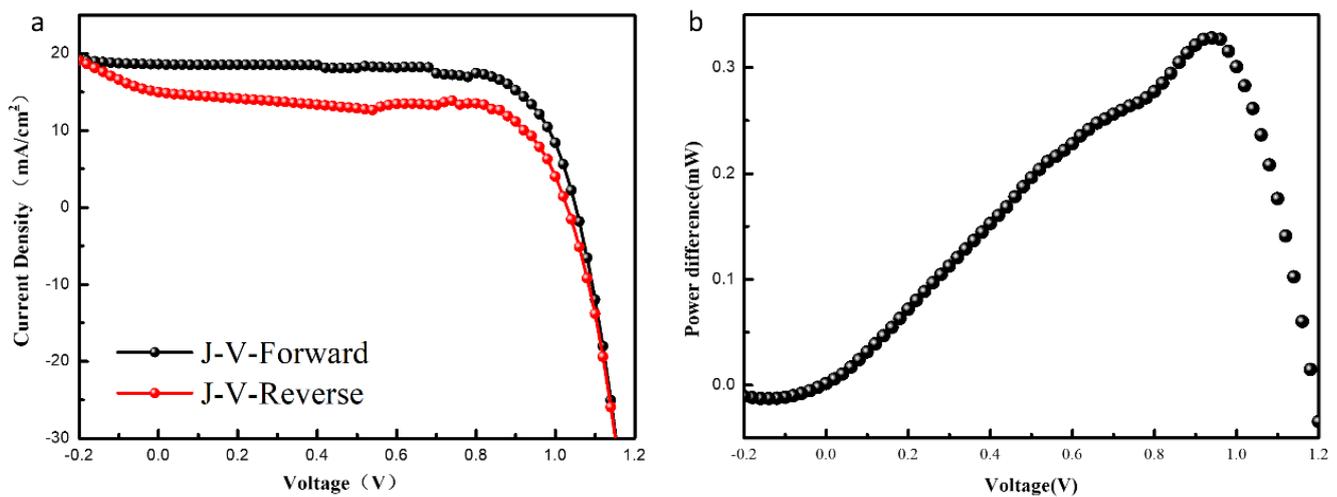
During the experiment, the 1 MΩ resistor was first connected to the circuit, the laser was turned on to form a perturbation, the background light intensity was adjusted to excite the battery to reach 0.1 V_{oc}, 0.3 V_{oc}, 0.5 V_{oc}, and 0.7 V_{oc}, respectively, and then the voltage dynamic was traced by the time-resolved oscilloscope. Subsequently, the 50 Ω resistor was connected to the circuit, the 1M Ω resistor was simultaneously disconnected from the circuit due to the channel control. Then the background light intensity was readjusted to the previous relative voltage condition, and the change in current can also be traced by the oscilloscope.

Fig. 2. (a) Cell forward and reverse sweep J-V curve, (b) Hysteresis power

3. Results and discussion

The forward and reverse scan *J-V* curves of MAPbl₃ perovskite solar cells with planar heterojunction structure prepared by two-step spin-coating method are shown in Fig. 2(a) The scanning rate was tuned from -0.2 V to 1.2 V for forward scanning and 1.2 V to -0.2 V for reverse canning. The voltage changes in step wide of 0.02 V rather than a pulse voltage signal. The stepwise scanning can decrease the transient voltage effect which will decrease the charging and discharging effect for the solar cells. In forward scanning mode, the measured short-circuit current was 1.498 mA, the open-circuit voltage was 1.051 V, the power was 1.15 mW, the fill factor was 71.9144%, leading to an efficiency of 14.2628%. Meanwhile, in the reverse sweep mode, the short-circuit current was 1.20 mA, the open-circuit voltage was 1.02V, the maximum power is 0.88 mW, the fill factor is 70.9951%, the efficiency is

10.9605%. Thus, the hysteresis index can be evaluated by equation of $(PCE^{+}-PCE^{-})/(PCE^{+}+PCE^{-})$.

The hysteresis index of perovskite cell was calculated to be 0.13. It can be seen that the planar heterojunction structure MAPbl₃ perovskite solar cell prepared by two-step spin-coating method demonstrated a strong hysteresis phenomenon, the maximum power point (MPP) measured in the reverse scanning mode was significantly decreased compared to the forward scanning mode. To better reflect the trend of hysteresis with voltage, we multiplied the current difference with the voltage to obtain the power difference from hysteresis, as shown in Fig. 2(b), where the power difference raised slowly from short circuit condition to MPP and then drops sharply at the MPP of 1 V.
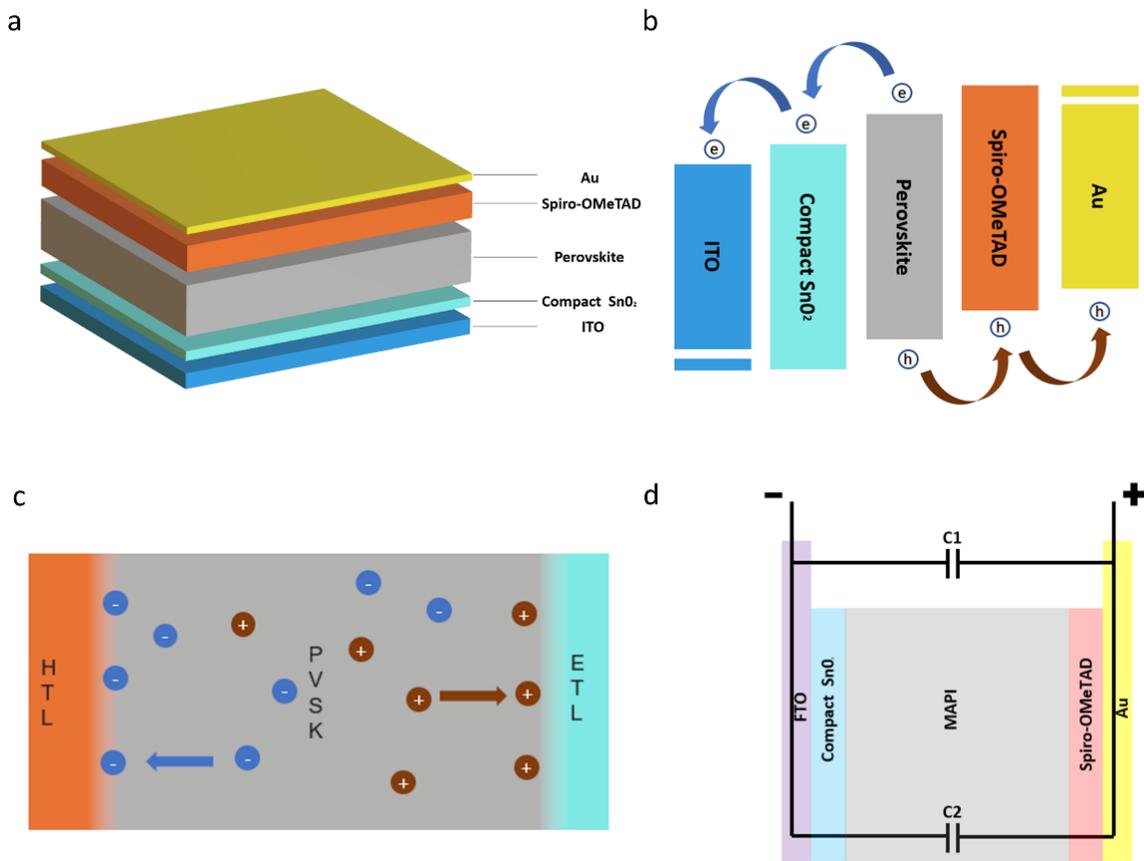
Fig. 3. (a) Structure of planar heterojunction perovskite solar cell, (b) Electron and hole movement in the cell, (c) Ion aggregation at the electron/hole transport layer boundary, (d) Simple electrical model of solar cell (color online)

As mentioned above, the ion migration has been widely recognized as the main factor of hysteresis. Fig. 3(a) provides the structure of $MAPbI_3$ perovskite solar cell with planar heterojunction structure, perovskite is the absorber layer, Spiro-OMeTAD is the hole transport layer (HTL), SnO_2 is the electron transport layer (ETL), and Au and ITO are the anode and cathode. Fig. 3(b) draws the schematic paths of holes and electrons moving inside the perovskite solar cell under background light. When the perovskite solar cell is illuminated, its internal perovskite absorber layer absorbs photons to generate electron-hole pairs, and then these carriers become free carriers or excitons and are collected by the electron transport layer and hole transport layer and finally extracted by the electrode. As shown in Fig. 3(c), when the cell is exposed to stable light or is applied with positive bias, the low dissociation energy of perovskite generates ions in active layer. The light induced ions are attracted by the high concentration of holes and electrons in the HTL and ETL to product the migration, where the cations moving toward the electron transport layer and the anions moving toward the hole transport layer. In Teng's model, I^- aggregates near the hole transport layer [6], while Azpiroz confirmed that MA^+ aggregates near the electron transport layer [30], that

confirmed our assumption. However, different like carriers, the size of ions was significant larger, resulting in accumulation of ions at each interface (cation at ETL/perovskite and anion at HTL/perovskite), respectively. The accumulation brought a change in the overall capacitance of the device. And based on the capacitance dynamic, a simple electrical model of a planar heterojunction perovskite solar cell can be drawn (Fig. 3(d)), where C_1 is the geometric capacitance of the cell and C_2 is the differential capacitance of the cell. The geometric capacitance comes from the geometry structure of the cell, and the value depends on the distance between the two plates, the area of the cell, and the dielectric constant of the substance between the two poles. On the other hand, the ion accumulation at interfaces, caused by ion migration, can also block the charge extraction. This blocking effect generated a novel capacitance only existed in perovskite, which is called differential capacitance. Since the differential capacitance originates from ion migration, its magnitude depends on the degree of ion migration. To extract differential capacitance, the TPV and TPC techniques were both performed for the following analysis.
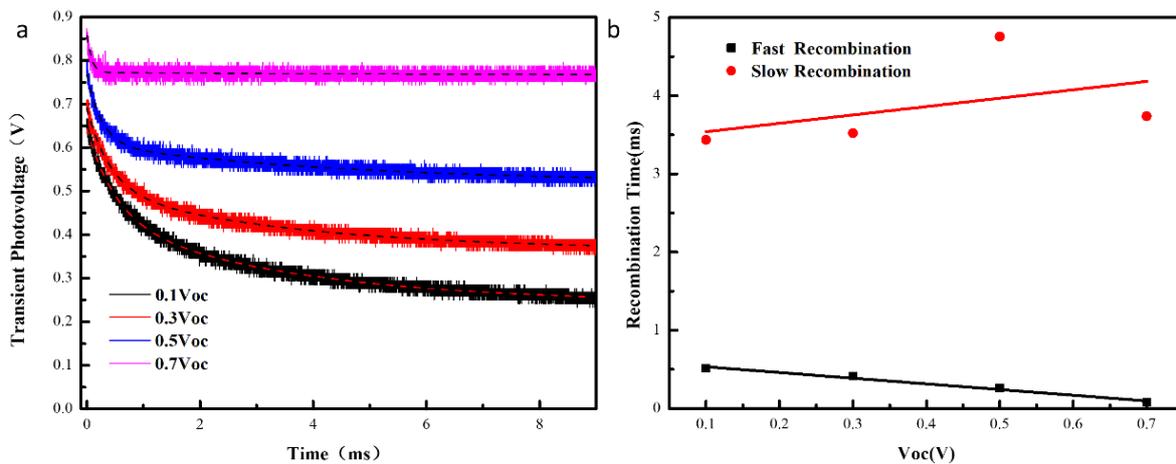
Fig. 4. (a) TPV test data and fitting results, (b) Charge recombination time (color online)

TPV technology can be used to dig the carrier recombination process in solar cells, Fig. 4(a) gives the results of the TPV decay in perovskite solar cells, where the dashed line is the result of an exponential nonlinear fit to extract the geminate and nongeminate recombination, the formula was $y=A_1*exp(-x/t_1)+A_2*exp(-x/t_2)+y_0$, t_1 and t_2 represent two recombination lifetimes, respectively. It can be seen, as V_{oc} increases, the effect of transient signal decreases to the V_{oc} dynamic, where the photovoltage transient decreased rapidly to stable state. Fig. 4(b) displayed the tendency of the two-recombination lifetime extracted from our fitting results. It can be seen that recombination types were changing differently along with the increasing background voltage bias. The geminate recombination was significantly accelerated, while the nongeminate recombination speed slightly increased along with the background voltage bias tuning. According to the previous introduction [21], the nongeminate was mainly caused by the ion migration and geminate recombination was controlled by the carrier recombination at open circuit condition. Obviously, when the injection was increased (higher background light), the number of electrons and holes were increased due to the photoconversion effect, the recombination possibility between electrons and holes was enlarged, leading to an increased geminate recombination rate. Meanwhile, the ion migration accumulated charges at interfaces which decreased the ion intensity inside of the perovskite bulk, resulting a decreased nongeminate recombination rate boundary, which marked ions cannot recombine with the charges that are uniformly distributed in the absorber layer and showed a slower rate of recombination.
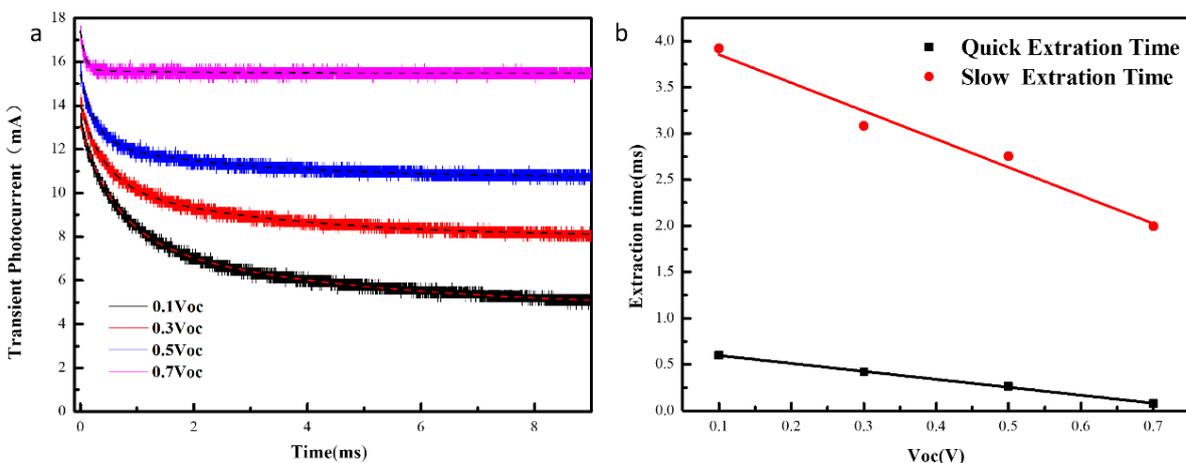

Fig. 5. (a) TPC test data and fitting results, (b) Charge extraction time (color online)

The TPC can trace the current dynamic at short condition and obtain the charge extraction of the cell. Fig. 5(a) showed the variation of the photocurrent dynamic under various background irradiation intensity. A nonlinear exponential fit was applied to the TPC result and the charge extraction rate can be extracted from the lifetime of

exponential formula. The charge extraction rates for different background light conditions are given in Fig. 5(b), it can be seen charge extraction rate increases with the background light intensity. Since the increase of light intensity, the internal electric field was also increased, which enlarges a dramatic ion migration rate as well.

As mentioned above, the carrier recombination rate and the carrier extraction rate can be analyzed by fitting the data of TPV and TPC. Further processing the data of TPV and TPC can reveal the detailed information of ion migration. As shown in Fig. 6(a), in the TPV data, the change in open-circuit voltage after pulsed laser injection

will result in a dynamic enhancement of the voltage ΔV. The ΔV varies with V_{oc} as shown in Fig. 6(b), the change in V_{oc} was decreased because of the increase of background light. Meanwhile, the TPC data can also be applied to calculate the charge inside the solar cell due to the definition of current

$$i = \frac{dQ}{dt} \qquad (1)$$

where Q is the total charge extracted from the pulse injection process, t is the time during the TPC measurement, and i was the current measured by TPC.
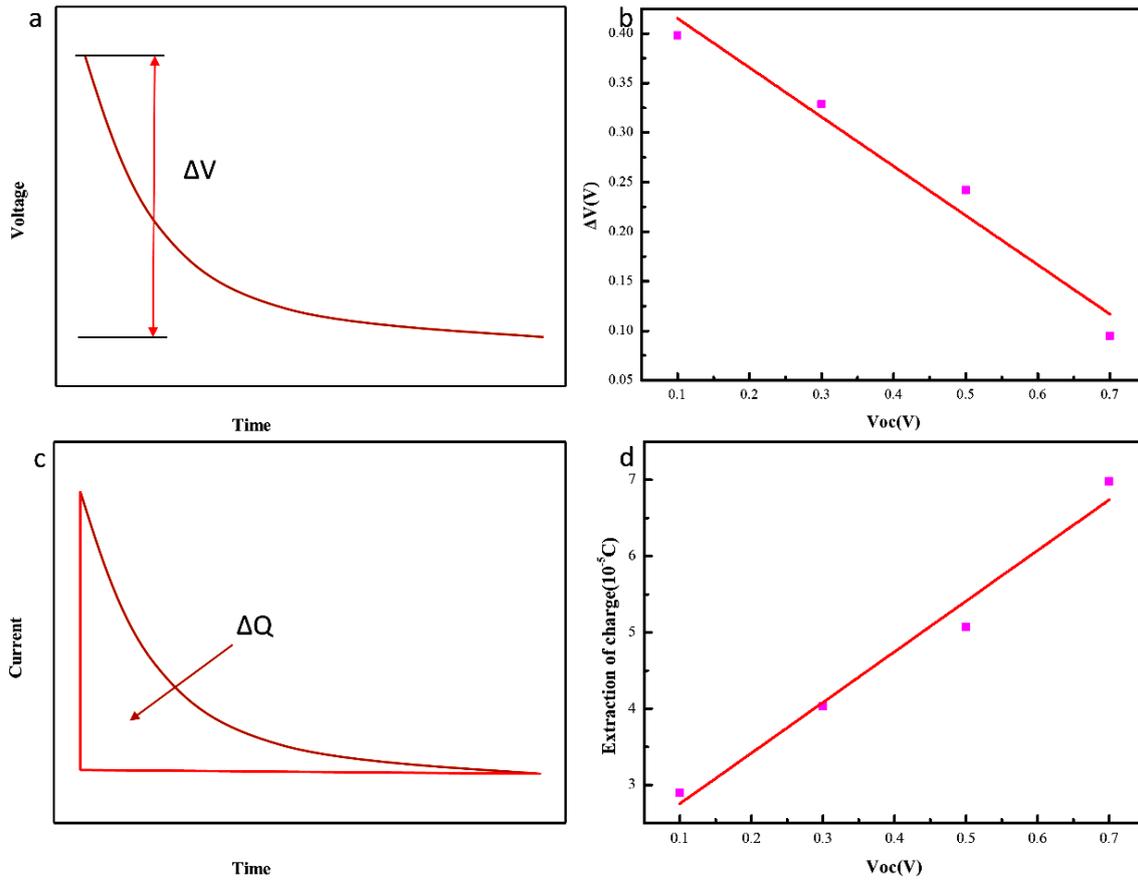

Fig. 6. (a) Schematic diagram of ΔV, (b) Values of ΔV for different Voc conditions, (c) Schematic diagram of ΔQ, (d) Extracted charge values under different Voc conditions

The extracted charge (ΔQ) was shown schematically as in Fig. 6(c). While the density of ΔQ was calibrated at different Voc and was summarized Fig. 6(d), it can be seen that the total charge extracted increased linearly with the increase of the background light. The reason for this phenomenon was that the increase of background light accumulated an increase in carrier concentration within the cell. Based on summarizing the TPV and TPC data, the change in voltage ΔV under open circuit conditions and the charge extracted under short circuit conditions ΔQ can be obtained. Meanwhile, in the external circuit, only the constant resistor was connected in parallel with the

perovskite solar cell during the TPV and TPC test. Thus, the charge of the open-circuit state can be approximated as equal to the charge extracted from the short-circuit state (ΔQ) The amount of change in the cell capacitance during the transient can be obtained by performing a calculation using the equation defining the capacitance, which is the value of the differential capacitance.

$$dC(Voc) = \frac{\Delta Q}{\Delta V} \qquad (2)$$

Hence, the differential capacitance calculated by measuring cells at different background light were given in

Fig. 7(a), and it can be seen that the differential capacitance had a significant increase with the linear raising of background light bias, and the magnitude of the differential capacitance depended on the degree of ion migration, it is clear that light had a facilitating effect on ion migration inside the perovskite solar cell.

After obtaining the differential capacitance, the total electrical $Q_{(bulk)}$ stored in the device also can be calculated by using the differential capacitance to integrate over Voc.

$$Q_{(bulk)} = \int_{0}^{Voc}[dC(Voc)]dVoc \tag{3}$$

As show in Fig. 7, the difference between the charge in bulk (Q_{bulk}) and transient charge (ΔQ) in TPC dynamic should be attributed to the ionic charge and the results was displayed Fig. 7(b). In perovskite materials, the halide cations and methyl-ammonium anions only carry single charge (I^- and MA^+), Hence we can extract the mole concentration in details for the ion migration inside of perovskite solar cells once the light intensity was up to 700 W/m^2, the concentration of ion migration was up to 5.72×10^{-6} mol/cm^2 in MAPbI$_3$ based perovskite solar cells. These ions accumulated at the boundary between the perovskite film and HTL /ETL, adsorbed electrons and holes, Hinder charge extraction and eventually cause the cell to exhibit a hysteresis effect.
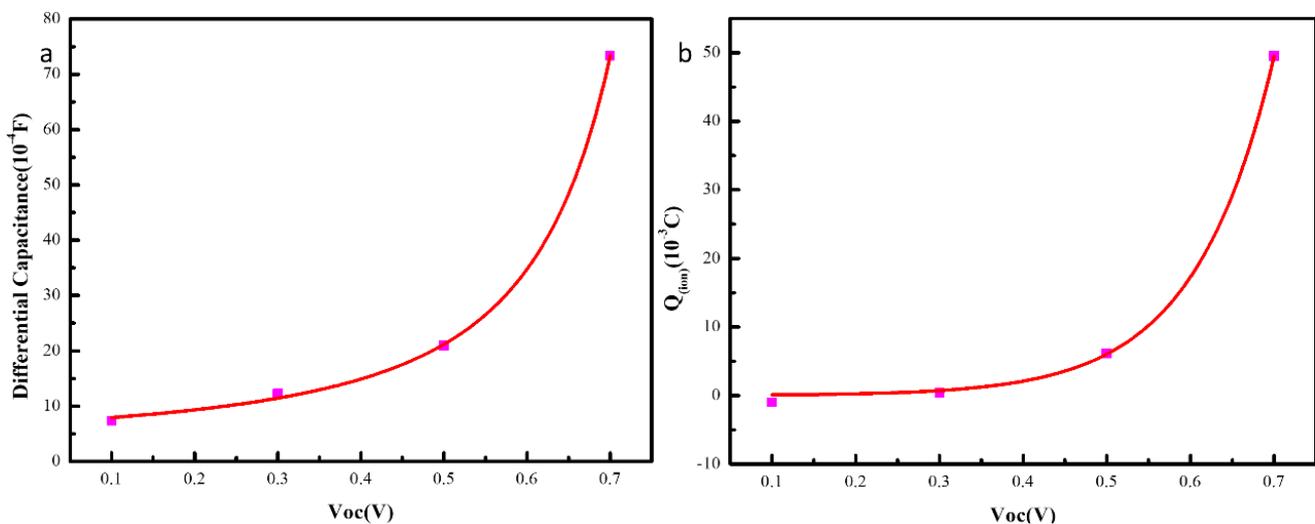

Fig. 7. (a) Differential capacitance values under different background light, (b) Total device charge values under different background light

4. Conclusion

The ion migration was found to be the main reason for the hysteresis in perovskite solar cells, and we have presented a non-contact method for characterizing the ion migration. Instead of measuring perovskite films, the TPV/TPC combined way can extract charge carriers inside of perovskite solar cells directly which also include the ionic charge. Hence, the focus of differential capacitance was introduced in this article for tracing the dynamic of ion migration. It can be found that the light irradiation was significantly related to the ion migration because the weak bonding energy in perovskites. Ions of MA^+ and I^- were dissociated under the photon injection and thus diffused to interfaces between perovskite active layer and functional layers. We designed dual light beam for the characterization of ion migration, the constant LED was applied to trigger the ion migration and the second pulse laser signal was applied to extract the ionic charge density

from photon current dynamic. We found that the tough the ion migration was tiny in mole concertation (low to 5.72×10^{-6} mol/cm^2 under 700 W/m^2), the hysteresis was significantly enhanced because the current was also related to the scanning time (i=dQ/dt). We have proposed a novel method for characterization the ionic density for perovskite solar cells which is significant for the evaluation of hysteresis effect in perovskite solar cells and thus can accelerate the development of industrialization of perovskite solar cells.

References

[1] A. Kojima, K. Teshima, Y. Shirai, T. Miyasaka, Journal of the American Chemical Society **131**(17), 6050 (2009).

[2] J. H. Im, C. R. Lee, J. W. Lee, S. W. Park, N. G. Park, Nanoscale **3**(10), 4088 (2011).

[3] J. J. Yoo, G. Seo, M. R. Chua, T. G. Park, J. Seo, Nature **590**(7847), 587 (2021).

[4] Y. Wu, H. Shen, D. Walter, D. Jacobs, T. Duong, J. Peng, K. Weber, Advanced Functional Materials **26**(37), 6807 (2016).

[5] Y. Zhou, F. Huang, Y. B. Cheng, A. Gray-Weale, Computational Materials Science **126**, 22 (2017).

[6] T. Zhang, C. Hu, S. Yang, Small Methods **4**(5), 1900552 (2019).

[7] C. C. Stoumpos, C. D. Malliakas, M. G. Kanatzidis, Inorganic Chemistry **52**(15), 9019 (2013).

[8] H. S. Kim, I. Mora-Sero, V. Gonzalez-Pedro, Nature Communications **4**, 2242 (2013).

[9] H. J. Snaith, A. Abate, J. M. Ball, Journal of Physical Chemistry Letters **5**(9), 1511 (2014).

[10] R. S. Sanchez, V. Gonzalez-Pedro, J. W. L. Ee, Journal of Physical Chemistry Letters **5**(13), 2357 (2014).

[11] E. L. Unger, E. T. Hoke, C. D. Bailie, Energy & Environmental Science **7**(11), 3690 (2014).

[12] R. Gottesman, E. Haltzi, L. Gouda, Journal of Physical Chemistry Letters **5**(15), 2662 (2015).

[13] A. Kumar, Optical and Quantum Electronics **53**(4), 1 (2021).

[14] Y. Li, J. Shi, B. Yu, B. Duan, J. Wu, H. Li, Joule **4**(2), 472 (2020).

[15] S. Meloni, T. Moehl, W. Tress, Y. H. Lee, Nature Communications **7**(1), 1 (2016).

[16] D. W. Miller, G. E. Eperon, E. T. Roe, C. W. Warren, H. J. Snaith, M. C. Lonergan, Applied Physics Letters **109**(15), 6050 (2016).

[17] M. T. Neukom, S. Züfle, E. Knapp, M. Makha, R. Hany, B. Ruhstaller, Solar Energy Materials and Solar Cells **169**, 159 (2017).

[18] E. L. Unger, E. T. Hoke, C. D. Bailie, W. H. Nguyen, A. R. Bowring, T. Heumüller, M. D. McGehee, Energy & Environmental Science **7**(11), 3690 (2014).

[19] Z. Kang, H. Si, M. Shi, C. Xu, W. Fan, S. Ma, Science China Materials **62**(6), 776 (2019).

[20] J. S. Yun, A. Ho-Baillie, S. Huang, S. H. Woo, Y. Heo, J. Seidel, Journal of Physical Chemistry Letters **6**(5), 875 (2015).

[21] M. Liu, Z. Chen, Z. Chen, H. L. Yip, Y. Cao, Materials Chemistry Frontiers **3**(3), 496 (2019).

[22] Y. Liu, N. Borodinov, M. Lorenz, M. Ahmadi, O. S. Ovchinnikova, Advanced Science **7**(19), 2001176 (2020).

[23] M. Liu, M. Endo, S. Ai, A. Wakamiya, Y. Tachibana, ACS Applied Energy Materials **1**(8), 3722 (2018).

[24] S. P. Malyukov, A. V. Sayenko, A. V. Ivanova, Materials Science and Engineering **151**(1), 012033 (2016).

[25] E. Palomares, N. F. Montcada, M Méndez, J Jiménez-López, W. Yang, G. Boschloo, "In Characterization Techniques for Perovskite Solar Cell Materials" Elsevier 161 (2020).

[26] J. W. Ryan, E. Palomares, Advanced Energy Materials **7**(10), 1601509 (2017).

[27] C. Brian, O'Regan, Piers, Journal of the American Chemical Society **137**(15), 5087 (2015).

[28] M. Miyashita, K. Sunahara, T. Nishikawa, Journal of the American Chemical Society **130**(52), 17874 (2008).

[29] J. Bisquert, F. Fabregat-Santiago, I. Mora-Seró, G. GarciaBelmonte, S. Giménez, The Journal of Physical Chemistry C **113**, 17278 (2009).

[30] J. M. Azpiroz, E. Mosconi, J. Bisquert, Energy & Environmental Science **8**(7), 2118 (2015).

_____

*Corresponding author: xi.xi@jiangnan.edu.cn